Proc. Natl. Acad. Sci. USA
Vol. 81, pp. 1594–1598, March 1984
Neurobiology

Diffusion and binding constants for acetylcholine derived from the falling phase of miniature endplate currents

(acetylcholine receptor/acetylcholine receptor kinetics/buffered diffusion/neuromuscular junction/saturated disk model)

BRUCE R. LAND†, WILLIAM V. HARRIS†, EDWIN E. SALPETER‡, AND MIRIAM M. SALPETER†

†Section of Neurobiology and Behavior, Division of Biology, and ‡Department of Physics, Cornell University, Ithaca, NY 14853

Contributed by Edwin E. Salpeter, November 28, 1983

ABSTRACT **In previous papers we studied the rising phase of a miniature endplate current (MEPC) to derive diffusion and forward rate constants controlling acetylcholine (AcCho) in the intact neuromuscular junction. The present study derives similar values (but with smaller error ranges) for these constants by including experimental results from the falling phase of the MEPC. We find diffusion to be 4×10^{-6} cm^2 s^{-1}, slightly slower than free diffusion, forward binding to be 3.3×10^7 M^{-1} s^{-1}, and the distance from an average release site to the nearest exit from the cleft to be 1.6 μm. We also estimate the back reaction rates. From our values we can accurately describe the shape of MEPCs under different conditions of receptor and esterase concentration. Since we suggest that unbinding is slower than isomerization, we further predict that there should be several short "closing flickers" during the total open time for an AcCho-ligated receptor channel.**

The vertebrate neuromuscular junction has a high concentration of acetylcholine receptors (AcChoR) and very rapid physiological response to single quantal packets of acetylcholine (AcCho). We have combined measurements from the time course of miniature endplate currents (MEPCs) and AChoR site densities, σ, with modeling of a standard kinetic scheme. The MEPC rising phase was discussed in previous papers (1, 2); the falling phase is discussed in the present paper. This allows us to derive the rate constants of diffusion and binding of AcCho and isomerization of the AcCho-activated ionic channel.

Recently, cation translocation studies and single-channel recordings (e.g., see refs. 3–6) have provided many kinetic parameters that predict MEPCs and single-channel wave forms. [For earlier values, see review by Heidmann and Changeux (7).] In our approach we use the shape of the MEPC as a function of AcChoR concentration to derive forward binding rates as well as information on AcCho diffusion in the intact neuromuscular cleft. We thus complement the results obtained by chemical techniques and by single-channel recording. The derived parameters support our motivating assumptions of the "saturating disk model" used by Salpeter and colleagues (8–11) to explain the generation of the MEPC.

METHODS

We recorded MEPCs by voltage clamp from the intercostal muscle of the lizard *Anolis carolinensis*, using experimental techniques as in the first two papers of this series (1, 2) with minor modifications.

Three groups were used: (*i*) control muscle (esterases and receptor concentration unaltered); (*ii*) receptors intact and esterases fully inactivated [with 1 mM diisopropyl fluorophosphate (iPr_2P-F) for 1 hr]; (*iii*) receptors partially inactivated [with 40 nM α-bungarotoxin (BTX) for 40 min] to $\approx$0.36 its normal value (papers 1 and 2) and esterases inactivated with iPr_2P-F as in *ii*. The filtering conditions of the voltage clamp were modified from those used in papers 1 and 2 to improve the signal-to-noise ratio. Because the falling phase of MEPCs is slow relative to the rise time, the signals were low-pass-filtered at 1 kHz (two-pole Butterworth filter) and the digitizer sampling rate was reduced to 6.25 kHz. Even though the Nyquist frequency is only a factor of 3 above our filter cutoff, aliasing was judged to be less than 4% of peak current. All experiments were done at 22 ± 1°C and −100 mV holding potential. Fall time (t_f) values were obtained from the experimental MEPC as 1.23 × the 90–40% fall time. The factor 1.23 is the conversion from 90–40% to *e*-folding time for a pure exponential.

RESULTS

Fig. 1 shows six examples of measured MEPC traces, illustrating the three conditions used in the present study. Fig. 2 plots the relation between t_f and MEPC amplitude A_c, and Table 1 gives the mean values of t_f and A_c under these conditions.

We confirm (12–15) that inactivation of esterases lengthens t_f appreciably and that, when σ is reduced by BTX treatment, t_f is somewhat shortened again (12, 15). Our additional observations are that, when esterases are intact, t_f does not depend on A_c (Fig. 2*A*), but after esterase inactivation t_f *increases* with increasing A_c (Fig. 2*B*). Finally, decreasing σ, with esterases inactivated, almost eliminates the correlation between t_f and A_c (Fig. 2*C*).

Chemical Kinetics Scheme

We first assume that AcCho is released instantaneously from a very small area and diffuses in the cleft with diffusion constant D. A standard chemical kinetics scheme (16) is then assumed for the interaction of AcCho with receptor at any point in the cleft:

$$2A + R_c \underset{k_{-1}}{\overset{2k_{+1}}{\rightleftharpoons}} A + AR_c \underset{2k_{-2}}{\overset{k_{+2}}{\rightleftharpoons}} A_2R_c' \underset{l_-}{\overset{l_+}{\rightleftharpoons}} A_2R_c^*, \qquad [1]$$

in which A is AcCho, A_2R_c' is the doubly bound AcChoR–channel complex in the closed conformation, and $A_2R_c^*$ is that complex in the open conformation. In this scheme we

The publication costs of this article were defrayed in part by page charge payment. This article must therefore be hereby marked "*advertisement*" in accordance with 18 U.S.C. §1734 solely to indicate this fact.

Definitions and abbreviations: AcCho, acetylcholine; AcChoR, acetylcholine receptor or single AcCho binding site; σ, AcChoR site density; R_c, AcChoR–channel complex—i.e., the unit consisting of the AcCho channel and the AcCho binding sites needed to activate it; iPr_2P-F, diisopropyl fluorophosphate; BTX, α-bungarotoxin; MEPC, miniature endplate current; A_c, MEPC amplitude; t_r, rise time; t_f, 1.23 × 90–40% fall time; N, number of AcCho molecules released per quantal packet; D, diffusion constant; R_{ex}, characteristic distance from release site to edge of receptor-containing cleft; g, fraction of doubly bound R_cs that are open; χ_-, effective unbinding rate (see Eq. 2).

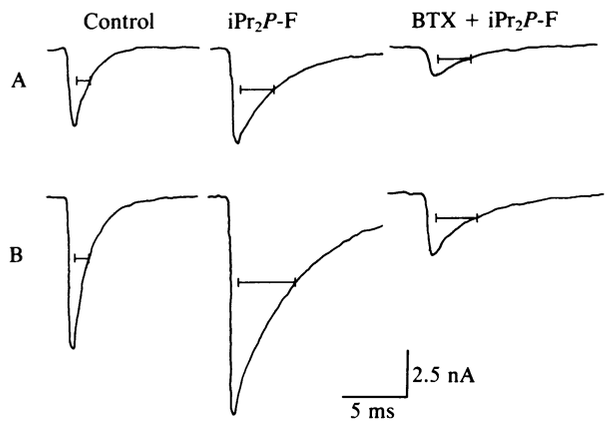

FIG. 1. Averaged MEPC traces of below (*A*) and above (*B*) mean amplitude for each of three experimental conditions (see *Methods*). Each trace is the average of some 100–400 individual MEPC recordings. The smaller traces (*A*) are ≈0.7 × mean A_c and the larger traces (*B*) are ≈1.4 × mean A_c. The bars extend from the 90% point to the 40% point in the falling phases. Note that iPr_2P-F-treated endplates produce longer and more amplitude-dependent MEPC fall times than either of the other two conditions (see also Fig. 2 and Table 1).

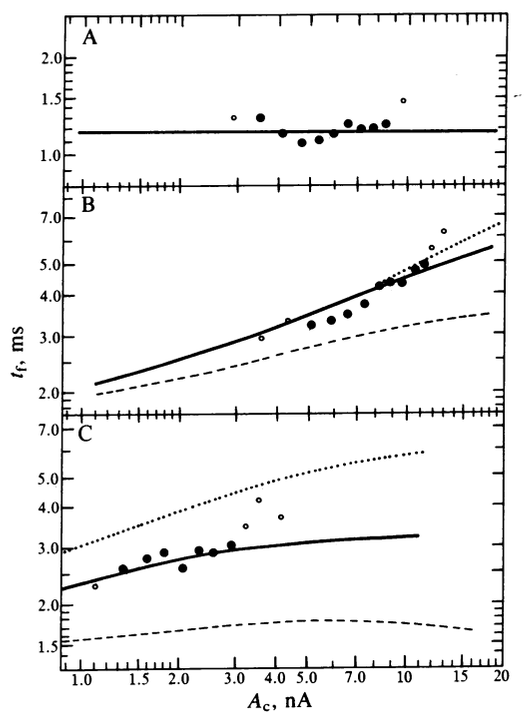

FIG. 2. Fall time vs. MEPC amplitude, showing both experimental points and model fits. Of the experimental points, ●s represent amplitude bins used in the data analysis (having >100 MEPCs). ∘s represent amplitude bins with few traces ($50 < n < 100$ MEPCs averaged). *A* shows that the MEPC fall times of control endplates (no iPr_2P-F or BTX) are independent of amplitude, whereas in *B* (iPr_2P-F-treated endplates) the t_f–A_c correlation is strong and in *C* (BTX + iPr_2P-F-treated endplates) it is still positive but somewhat reduced. The model curves refer to quantities χ_- and R_{ex} defined in the text. The horizontal (model) line in *A* corresponds to $1/\chi_-$. *B* compares data with three computed model curves with various distances R_{ex}: heavy curve for best value of $R_{ex} = 1.6$ μm, using Table 2 parameters; dotted curves for $R_{ex} = 2.2$ μm; and broken curve for $R_{ex} = 1.1$ μm (all other model parameters kept constant). Note that the computed curves for $R_{ex} \geq 1.6$ μm are relatively close together, so that the model fit to iPr_2P-F data is relatively insensitive to large R_{ex}. *C* compares model curves with experimental data, as explained for *B*. It shows that when σ is reduced the fit is very sensitive to R_{ex}.

Table 1. Experimental results for amplitude A_c and fall time t_f

Conditions	No. traces	A_c, nA	t_f, ms
Esterases intact	2224	6.1 ± 0.8	1.16 ± 0.05
iPr_2P-F	3877	7.9 ± 1	4.0 ± 0.2
BTX + iPr_2P-F	1003	2.2 ± 0.4	2.8 ± 0.2

The error ranges given are the statistical standard errors, plus an estimate for systematic measurement errors.

assume that there are two AcChoR binding sites per channel complex (R_c), that both sites have to be occupied by AcCho to allow the opening of the channel, and that unbinding can occur only from the closed conformation. This scheme contains (in addition to the diffusion constant *D*) six parameters: two binding constants (k_{+1} and k_{+2}), two unbinding constants (k_{-2} and k_{-1}), and two rate constants for a conformational change, l_+ for channel opening and l_- for channel closing. (The k_+ and k_- constants are for the individual binding sites of the two-site channel complex.) By varying σ experimentally (1, 2) we had subdivided the MEPC rise time, t_r, into a σ-dependent "reduced rise time" and a σ-independent time contribution that gives a lower limit to the relaxation rate for gating, $(l_+ + l_-) \approx 25\ ms^{-1}$. We assume throughout the present paper that there is no "direct cooperativity" in either the binding step or the unbinding step, so that $k_{+1} = k_{+2} \equiv k_+$; and $k_{-1} = k_{-2} \equiv k_-$ (we will discuss results for different assumed ratios of these values elsewhere). Because it is not easy to get a value for k_- independent of l_-, we shall use an abbreviated chemical kinetics scheme that omits the gating delay and combines isomerization constants with the unbinding constants $2k_{-2}$:

$$2A + R_c \underset{k_-}{\overset{2k_+}{\rightleftharpoons}} A + AR_c \underset{\chi_-}{\overset{k_+}{\rightleftharpoons}} A_2R_c, \qquad [2]$$

in which $k_+ \equiv k_{+1} = k_{+2}$; $A_2R_c = A_2R'_c + A_2R^*_c$ refers to any doubly bound complex (open or closed) and χ_- is an effective unbinding rate. We define $g = A_2R^*_c/A_2R_c$ as the fraction of doubly bound receptor complexes with an open channel. At isomerization equilibrium in Eq. **1**, the ratio $g/(1-g)$ of open to closed channels is l_+/l_- and g is $l_+/(l_+ + l_-)$. We shall argue for the assumption $k_- < l_+ + l_-$, in which case isomerization equilibrium is maintained during the falling phase. Because unbinding can occur only from the closed state, the effective unbinding rate χ_- in Eq. **2** is related to the rate k_{-2} in Eq. **1** by

$$\chi_- = (1-g)2k_{-2} = \frac{l_-}{l_+ + l_-}\, 2k_{-2}. \qquad [3]$$

Thus, although we assume the absence of any "direct cooperativity" between k_{-1} and k_{-2}, we have the "apparent cooperativity" implied by $\chi_- < 2k_-$ (see also ref. 6).

Qualitative Predictions of Saturated Disk Model

Before discussing results of numerical modeling of diffusion plus the scheme in Eq. **2**, we describe some qualitative features and inequalities. Following the terminology of Land *et al.* (1, 2), we define three quantities, a_q, $2t_d$, and t_b. The postsynaptic quantal area ($a_q = N/\sigma$) is that area containing a number of AcCho binding sites equal to the number of AcCho molecules in the released quantal packet (*N*). The time $2t_d = (0.8/4\pi) \times (N/\sigma D)$ [equation 3 of Land *et al.* (2)] is the characteristic time for released AcCho to diffuse over area a_q without binding; $t_b = 0.93\ h/(\sigma k_+)$ [equation 4 in Land *et al.* (2)] is the characteristic time for a single AcCho molecule to bind in the presence of excess receptor (h is the width of the cleft). By "saturating conditions" we mean that

(σ/h), the AcCho concentration that a quantal packet would have in the cleft over area a_q, is large compared with the dissociation constant K_d ($= k_-/k_+$). If, in addition to saturating conditions, we also had $t_b < 2t_d$, then we would obtain a "saturated disk" of area a_q (where most receptor–channel complexes will be doubly bound) surrounded by a rim a_r of partially bound complexes. Because of excess receptors in the rim, the time that an AcCho molecule is free to diffuse is t_b, and the area of the rim $a_r \approx (t_b) \times (D)$. From the definition of $t_d \approx a_q/2D$ we have

$$a_r/a_q \approx t_b/2t_d. \quad [4]$$

Unlike the rising phase (10, 11), the events associated with the falling phase of the MEPC should depend strongly on the presence of esterases. In the case in which all esterases are intact, no (or little) repeated binding is expected (17). The MEPC will then decay exponentially as $e^{-(\chi_- t)}$. Thus χ_- (the "apparent unbinding rate" in Eq. 2) is the inverse of the fall time with esterases intact. In the absence of esterases, the AcCho molecules released from receptors diffuse for a time of order t_b until they rebind to receptors, where they again stay a time $1/\chi_-$ or the "apparent unbinding time." The only net change after such an AcCho "hopping cycle" in this process of "buffered diffusion" (12) is that the bound AcCho molecules are spread over an area larger by the rim a_r (Eq. 4). After H successive "hops," the quantal packet has spread over an area of about $a_q + (H)(a_r)$. When $(H)a_r = a_q$, the AcCho will have spread over an area $2a_q$ and the MEPC amplitude will have fallen to half its peak value (due mainly to the number of AcCho molecules ineffective on singly ligated R_cs). The fall time in the absence of esterases is therefore the duration of one hopping cycle [given by the fall time with esterases intact ($1/\chi_-$)] multiplied by the number of hops (H) needed to reach $2a_q$ (i.e., when $H = a_q/a_r = 2\,t_d/t_b$ from Eq. 4). Therefore, in the absence of esterases:

$$t_f \approx \frac{2t_d}{t_b} \times \frac{1}{\chi_-} \approx \frac{0.069}{h} \times \frac{gNk_+}{gD} \times \frac{1}{\chi_-}. \quad [5]$$

Thus the falling phase, with and without esterases, provides a means of deriving k_+/D distinct from that previously obtained from the rising phases (2).

Since $t_f \propto N$ (Eq. 5) and since A_c increases with N [equation 2 of Land *et al.* (2)], the model predicts that when esterases are inactive there should be a positive correlation between t_f and A_c. Since there is a natural variation in N among quantal packets, such a correlation can be seen in our experiments (Fig. 2*B*).

According to Eq. 5, t_f should be independent of σ, but we must now introduce a correction that becomes appreciable when σ is small, namely, the loss of AcCho due to exit from the primary cleft (see also ref. 12). We model this loss by stipulating that any free AcCho disappears from the cleft when it has penetrated a radial distance R_{ex} from the source, and we consider R_{ex} as an adjustable parameter. We shall see that the area πR_{ex}^2 is much larger than $a_q = N/\sigma$ for the σ in the intact neuromuscular junction [15,000 sites per μm^2 (2)]. However, when σ is decreased appreciably with BTX treatment, and especially for large N, a_q approaches πR_{ex}^2. In that case the loss of AcCho from the cleft causes t_f to decrease. The extent of this effect under our experimental conditions is illustrated by the three theoretical curves corresponding to different values of R_{ex} in Fig. 2 *B* and *C*: in Fig. 2*B* varying R_{ex} has relatively less effect on the curves than in Fig. 2*C*, where the curve is depressed radically for large A_c and small R_{ex}.

Fitting the Model Parameters

In ref. 2 we analyzed the data for the rising phase without including any back reactions (replacing the unbinding constants k_- and χ_- in Eq. 2 by zero). From the measured *mean* reduced rise time and mean amplitude (and the measured σ for the intact neuromuscular junction) we found one relationship between k_+ and gD. In the present study we can derive an accurate value for χ_- and a range of values for k_- from t_f, thus allowing us to include a consideration of the back reactions.

As suggested above, if esterases are fully efficient, $\chi_- = 1/t_f$. Since the esterases cannot be 100% efficient in preventing AcCho hopping, our experimental value for $t_f = 1.16$ ms (Table 1) gives a lower limit to χ_-, so that $\chi_- \geq 0.86\ ms^{-1}$. Yet experimentally we see no evidence for hopping: if hopping were important, there would be a positive correlation between t_f and A_c. None is seen in Fig. 2*A*. Similarly, Anderson and Stevens (17) see no discrepancy in values for channel closing and current fall time when esterases are intact. We estimate measurement errors in these two experiments of at most about 30%. We thus carry out model fittings for values of χ_- of both the lower limit of $0.86\ ms^{-1}$ and an upper limit of $1.3 \times 0.86\ ms^{-1}$. With χ_- fixed, we modeled MEPC shapes for the kinetic scheme in Eq. 2 plus AcCho diffusion for many choices of gD, k_+, k_-, and gN. The main results for each computation are values for A_c, t_f, and t_r.

With χ_- fixed, the parameters g and k_- are related uniquely by Eq. 3. If we assume a value for either g or k_-, model fitting to the experimentally obtained values for A_c and t_f from the present study and t_r from ref. 2 will give k_+, D, and N. At present we can establish only a range for g (and k_-) on the basis of the following two arguments: (*i*) Each computer calculation gives, in addition to values for A_c, t_f, and t_r, the shape of the MEPC falling phase. For normal σ this shape depended somewhat on $1 - g$ as illustrated in Fig. 3. The

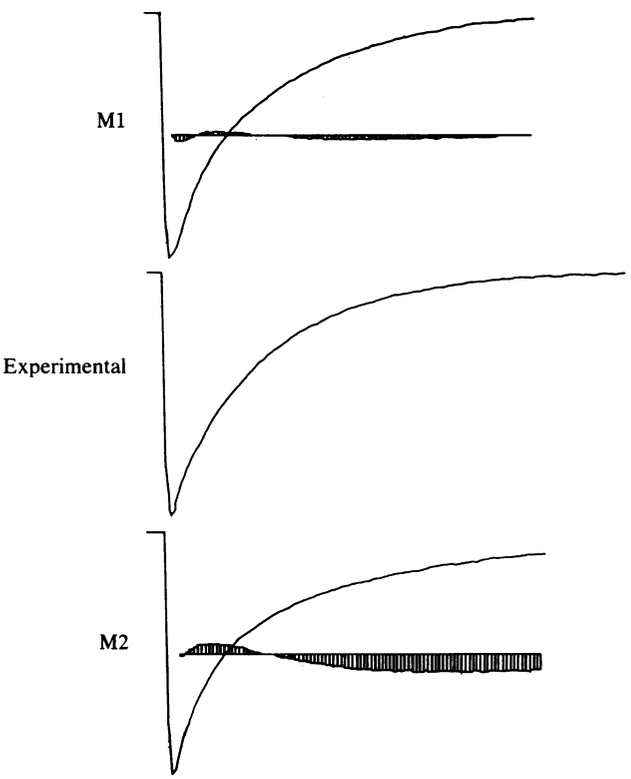

FIG. 3. Model and experimental MEPC waveforms. The trace labeled Experimental is the average of all MEPCs recorded in iPr_2P-F (at this time scale the rising phase carries no information). The two model traces M1 and M2 are for $(1 - g) = \chi_-/2k_- = 0.2$ (M1) or 0.5 (M2). Shaded curves are experimental minus model MEPCs. The fit is good for model M1 and generally for $(1 - g) \leq 0.2$ (3% rms error). The relatively poor fit (16% rms error) in model M2 gets progressively worse for $(1 - g) > 0.5$.

predicted and observed MEPC falling phase are in reasonable agreement only if $(1 - g) < 0.5$. (*ii*) If we assume an upper limit of ≈50 μM for $K_d = k_-/k_+$ as often suggested (6, 16, 18–23), our previously derived value for k_+ (2) gives $k_- < 5$ ms^{-1} and thus $(1 - g) > 0.1$. We therefore adopt a value for $1 - g$ between 0.1 and 0.5 and for k_- between 0.7 and 5 ms^{-1}. Possibilities of larger values for K_d and k_- will be analyzed in a later paper (see also Table 2).

For several values of k_- within the above range and for each of many assumed values of k_+/gD we carried out model calculations solving a coupled set of differential equations for diffusion and binding similar to Wathey *et al.* (24). Model fitting to observed A_c gives gN, and to the observed rise time (taken from ref. 2) gives gD and k_+ through the following empirical relation:

$$0.62(3.27/k_+) + 0.36(3.9/gD) = 1 \pm 0.15 \qquad [6]$$

with k_+ in units of 10^7 M^{-1} s^{-1} and D of 10^{-6} cm^2 s^{-1}. To obtain k_+ and gD from Eq. **6** uniquely, we still need the ratio k_+/gD, which is related to the ratio of t_f without and with esterases (see Eq. **5**) and is obtained from the model fitting to the experimental t_f. Finally, we found that the computed relation between t_f and k_+/gD has a weak dependence on the assumed value for R_{ex} when σ is normal (Fig. 2*B*) and a strong dependence when σ is reduced by BTX treatment (Fig. 2*C*). Fitting the computations to the measured t_f for *both* experimental conditions (by a rapidly converging iteration process) thus refines k_+/gD and gives R_{ex}. Results are given in Table 2.

Observational Checks for Model Parameters

We had determined all the parameters in Table 2 (with an assumption of $k_{-1} = k_{-2}$ and $k_{+1} = k_{+2}$) using only the *mean* values for t_r and t_f but not their A_c dependency. We now have a number of observational checks: (*i*) in paper 2 the t_r–A_c correlation gave a logarithmic slope $\beta = 0.5 \pm 0.25$. As explained in that paper, the theoretical value of β depends on the ratio k_+/gD. In the present paper we made an independent determination of k_+/gD entirely from the falling phase, and from this we calculated a value of $\beta \approx 0.30$, which is within our previously observed range of β. (*ii*) Similarly, the kinetic parameters give a calculated slope for the t_f–A_c relation that fits the experimental results (Fig. 2 *B* and *C*). (*iii*) Because of the "receptor hopping," one might expect the MEPC amplitude to decrease as t^{-1} for large time t. Yet for our adopted values of R_{ex} and $1 - g$, the calculated shape of the falling phase is almost exponential, as is the experimental shape (see Fig. 3).

Table 2. Kinetic parameters

k_{+1}	$= k_{+2} \equiv k_+ = (3.3 \pm 0.7) \times 10^7$ M^{-1} s^{-1}
χ_-	$= 0.86$ (+0.25, −0.05) ms^{-1}
$1 - g$	$= \chi_-/2k_- = 0.1$–0.5
k_{-1}	$= k_{-2} \equiv k_- \equiv (0.7$–$5.5)$ ms
l_+	$= (g) \times (25 \pm 10)$ ms^{-1}
l_-	$= (1 - g) \times (25 \pm 10)$ ms^{-1}
gD*	$= (2.7 \pm 0.8) \times 10^{-6}$ cm^2 s^{-1}
gN*	$= 6800 \pm 1400$
R_{ex}	$= 1.6 \pm 0.3$ μm

Stated error ranges are estimated standard errors obtained from the square root of sum of squares of individual experimental errors. Final accuracy in l_+, l_-, D, and N is further limited by uncertainty in g (≈0.5–0.9). Furthermore, if either gD or k_+ is given, then Eq. **6** gives the other parameter more accurately than given in this table.
*To calculate N and D we need a value for single-channel conductance γ (see equations 2 and 3 of ref. 2). In this paper we used γ = 55 pS, the value given by Hoffmann and Dionne (25) for the temperature used in the present study (22°C), but for snake endplates. If γ for the lizard should turn out to be different, the values of D and N in this table should both be multiplied by (55 pS/γ). If one should accept larger values of K_d and k_- or [$(1 - g) < 0.1$] then the value for k_+ would be multiplied by the correction factor $(l_+ + k_-)/l_+$ (26).

DISCUSSION

Kinetic Parameters. The main results of our present series of papers are the numerical values for nine parameters in Table 2: the six chemical kinetics parameters for the scheme in Eq. **1**, the diffusion constant D, the distance R_{ex} to the exit from the cleft, and the mean number N of AcCho molecules per quantal packet. The equality of k_{+1} and k_{+2} in Table 2 is an assumption. The consequences of other values of the ratio k_{+1}/k_{+2} will be discussed in a later paper. We expect that postulating a much larger value of either k_{+1} or k_{+2} [which may be the case for carbamoylcholine (27)] will change the other parameters in Table 2 by factors of at most 2.

Even though we assume $k_{-1} = k_{-2}$, there is an apparent cooperativity in unbinding—unbinding from A_2R_c appears slower than from AR_c, because unbinding can occur only from the closed state. Thus the fraction of doubly bound closed channels, $1 - g = 0.1$–0.5, can be thought of as the "factor of effective cooperativity." The effective dissociation constant χ_-/k_+ is then lower than $k_-/2k_+$ by the same factor.

In paper 2 we omitted back reactions and derived values for the parameters k_+, gD, and gN from the rising phase alone. In the present study we include back reactions and the falling phase. The ratio of fall times with and without esterases gives us an independent value for the ratio k_+/gD that is gratifyingly close to that obtained in paper 2. Furthermore, although the parameters k_- and $(1 - g)$ are uncertain, the effective unbinding rate χ_- is known quite accurately. Thus the model fitting (being relatively insensitive to k_-) gives values for k_+, gD, and gN with improved accuracy compared with those in paper 2 but within the previously derived ranges.

The diffusion rate constant is somewhat smaller than that for free diffusion [given as 6–10×10^{-6} cm^2 s^{-1} (28–30)]. The value for N fits well with the experimentally derived upper limit of 10,000 from Kuffler and Yoshikami (31).

Escape Route from Cleft. Finally, a value of importance in determining the shape of the MEPC falling phase is R_{ex}, the typical distance from release site to edge of the cleft. Model fitting gave R_{ex} to be 1.6 μm. To test this morphologically we measured the length of the primary cleft from 65 axonal end boutons, obtained from nine different animals. The average *half-length* of the primary cleft was 2.6 μm, and the distance down the folds containing significant receptor is ≈0.25 μm (8, 32). It is gratifying that our model value for R_{ex} falls between these two limits.

Predictions for Single-Channel Recordings. Since l_+ is larger than $2k_-$ (Table 2), we predict that the single channels total open time of about 1.2 ms (at 22°C) will be interrupted by several brief closing gaps or "flickers," during which no unbinding of AcCho would occur. The mean number of such closings should be $l_+/2k_-$, ≈1.5–10, the mean duration of each individual "closed-state spike" would be only l_+^{-1}, ≈60 μs, and each "open spike" $l_-^{-1} \approx$ 50–600 μs. Several studies (e.g., refs. 3 and 33), but not all (ref. 4), show such multiple closings, thus verifying qualitatively our assertion that isomerization is more rapid than unbinding.

Buffered Diffusion. The pioneering paper by Katz and Miledi (ref. 12; see also ref. 15) developed the concept of "buffered diffusion" for the falling phase of a MEPC in the absence of esterases. They defined a ratio $(1 - p)/p$ of unbound to bound molecules. In our notation this equals the ratio of t_b, the time molecules are free to diffuse (2), to $1/\chi_-$,

the time to unbind. From data on the rising phase (2) we now have direct estimates for t_b and thereby calculate p to be ≈ 0.95 for normal σ and 0.85 after BTX treatment. Katz and Miledi had to assume much smaller values of p than our measured values to account for the large drop in MEPC amplitude when σ is decreased. However, this is no longer needed, since evidence is now strong that 2 AcCho molecules are required to open a channel (e.g., refs. 1, 10, 16, and 34–36). This can account for the drop in amplitude due to wastage of AcCho on partially blocked receptor complexes (1, 10, 11, 27).

We thank Sir Bernard Katz, Henry Lester, Paul Adams, and Vincent Dionne for helpful suggestions and Patricia Scattergood for typing the manuscript. This work was supported by Grant NS 09315 from The National Institutes of Health.

1. Land, B. R., Salpeter, E. E. & Salpeter, M. M. (1980) *Proc. Natl. Acad. Sci. USA* **77**, 3736–3740.
2. Land, B. R., Salpeter, E. E. & Salpeter, M. M. (1981) *Proc. Natl. Acad. Sci. USA* **78**, 7200–7204.
3. Colquhoun, D. & Sakmann, B. (1981) *Nature (London)* **294**, 464–466.
4. Dionne, V. E. & Leibowitz, M. D. (1982) *Biophys. J.* **39**, 253–261.
5. Adams, P. (1983) in *Myasthenia Gravis*, eds. Albuquerque, E. X. & Eldefrawi, A. T. (Chapman & Hall, New York), pp. 131–153.
6. Hess, G. P., Cash, D. J. & Aoshima, H. (1983) *Annu. Rev. Biophys. Bioeng.* **12**, 443–473.
7. Heidmann, T. & Changeux, J.-P. (1978) *Annu. Rev. Biochem.* **47**, 317–357.
8. Fertuck, H. C. & Salpeter, M. M. (1976) *J. Cell Biol.* **69**, 144–158.
9. Matthews-Bellinger, J. & Salpeter, M. M. (1978) *J. Physiol. (London)* **279**, 197–213.
10. Salpeter, M. M. & Land, B. R. (1980) in *La Transmission Neuromusculaire: Les Médiateurs et le "Milieu Intérieur,"* Fondation Singer-Polignac (Masson, Paris), pp. 101–110.
11. Salpeter, M. M. (1983) in *Myasthenia Gravis*, eds. Albuquerque, E. X. & Eldefrawi, A. T. (Chapman & Hall, New York), pp. 105–129.
12. Katz, B. & Miledi, R. (1973) *J. Physiol. (London)* **231**, 549–574.
13. Gage, P. W. & McBurney, R. N. (1975) *J. Physiol. (London)* **244**, 385–407.
14. Hartzell, H. C., Kuffler, S. W. & Yoshikami, D. (1975) *J. Physiol. (London)* **251**, 427–463.
15. Cull-Candy, S. G., Miledi, R. & Uchitel, O. D. (1980) *Nature (London)* **286**, 500–502.
16. Adams, P. R. (1981) *J. Membr. Biol.* **58**, 161–174.
17. Anderson, C. R. & Stevens, C. F. (1973) *J. Physiol. (London)* **235**, 655–691.
18. Neumann, E. & Chang, H. W. (1976) *Proc. Natl. Acad. Sci. USA* **73**, 3994–3998.
19. Adams, P. R. & Feltz, A. (1980) *J. Physiol. (London)* **306**, 283–306.
20. Cash, D. J., Aoshima, H. & Hess, G. P. (1981) *Proc. Natl. Acad. Sci. USA* **78**, 3318–3322.
21. Sheridan, R. E. & Lester, H. A. (1977) *J. Gen. Physiol.* **70**, 187–219.
22. Adler, M., Albuquerque, E. X. & Lebeda, F. J. (1978) *Mol. Pharmacol.* **14**, 514–529.
23. Lester, H. A., Koblin, D. D. & Sheridan, R. E. (1978) *Biophys. J.* **21**, 181–194.
24. Wathey, J. C., Nass, M. M. & Lester, H. A. (1979) *Biophys. J.* **27**, 145–164.
25. Hoffmann, H. M. & Dionne, V. E. (1983) *J. Gen. Physiol.* **81**, 687–703.
26. Sakmann, B. & Adams, P. R. (1978) in *Advances in Pharmacology and Therapeutics*, ed. Jacob, J. (Pergamon, Oxford), Vol. 1, pp. 81–90.
27. Sine, S. M. & Taylor, P. (1980) *J. Biochem.* **255**, 10144–10156.
28. Eccles, J. C. & Jaeger, J. C. (1958) *Proc. R. Soc. London Ser. B* **148**, 38–56.
29. Krnjevic, K. & Mitchell, J. F. (1960) *J. Physiol. (London)* **153**, 562–572.
30. Dionne, V. E. (1976) *Biophys. J.* **16**, 705–717.
31. Kuffler, S. W. & Yoshikami, D. (1975) *J. Physiol. (London)* **251**, 465–482.
32. Salpeter, M. M., Smith, C. D. & Matthews-Bellinger, J. (1984) *J. Electron Microsc. Tech.* **1**, 63–81.
33. Auerbach, A. & Sachs, F. (1983) *Biophys. J.* **42**, 1–10.
34. Adams, P. R. (1975) *Pflügers Arch.* **360**, 145–153.
35. Neubig, R. R. & Cohen, J. B. (1979) *Biochemistry* **24**, 5465–5475.
36. Colquhoun, D. (1979) in *The Receptors: A Comprehensive Treatise*, ed. O'Brien, R. D. (Plenum, New York), Vol. 1, pp. 93–134.